9. P. J. Morris and C. K. W. Tam, "Near and far fields noise from large-scale instability of axisymmetric jets," AIAA Pap., No. 77-1351 (1977).
10. N. M. Terekhova, "Stability characteristics of a supersonic jet in a co-current flow," Izv. Sib. Otd. Akad. Nauk SSSR Ser. Tekh. Nauk, 1, No. 4 (1986).
11. G. N. Abramovich, Theory of Turbulent Jets [in Russian], Fizmatgiz, Moscow (1960).
12. G. L. Morrison and D. K. McLaughlin, "Instability of supersonic jets at low Reynolds numbers," AIAA J., 18, No. 7 (1970).
13. N. A. Zheltukhin and N. M. Terekhova, "Modeling large-scale mixing processes in an expanding supersonic jet," Zh. Prikl. Mekh. Tekh. Fiz., No. 1 (1987).

RESONANCE FLOW RANDOMIZATION IN THE K-REGIME OF BOUNDARY-LAYER TRANSITION

S. V. Dryganets, Yu. S. Kachanov, V. Ya. Levchenko, and M. P. Ramazanov

UDC 532.536

Introduction. The empirical data presently available indicates the existence of two main regimes for the nonlinear disintegration of laminar flow in a boundary layer during the origination of turbulence. A survey of studies devoted to discovering and investigating these regimes and analyzing the reasons for their differences can be found in [1, 2]. The first regime is characterized by pulsations of characteristic bumps on the oscillograms at a certain stage of development of the instability wave. These bumps are generally regarded as corresponding to the beginning of the development of turbulence spots. This regime was first observed more than 30 yrs ago in experiments conducted at the National Bureau of Standards (USA) and was described in detail in [3]. In recognition of one of the authors of this study (Klebanov) and the fact that this regime has made an important contribution to the study of the transition to turbulence, it has been given the name "K-regime."

In 1976 investigators discovered a new, essentially different transition regime not characterized by the above-mentioned bumps or any of the other features associated with the K-regime [4]. The transition to turbulence in this regime occurred through a fairly smooth increase in the higher harmonics of the main instability wave, the appearance of a broad packet of low-frequency pulsations in the spectrum (including the subharmonic of the main wave), and their subsequent interaction and filling of the entire spectrum [4] (also see [5]).

The existence of two main transition regimes was confirmed by visualization of the perturbation field in a boundary layer in [6, 7]. It was shown in [8] that one regime is replaced by the other. Soon afterward [9, 10], it was explained that the main mechanism responsible for the development of a three-dimensional flow and randomization of the flow in the new transition regime is subharmonic parametric resonance of the plane main wave (of frequency ω_1) and three-dimensional stochastic background pulsations of the broad continuous spectrum within the region of the frequency of the subharmonic $\omega_{1/2} = \omega_1/2$. A mathematical model of this interaction in a triplet (low-mode) approximation was first proposed in [11, 12]. A weakly linear theory of the formation of the new regime which quantitatively describes experimental observations was constructed in [13, 14]. Due to the determining role of subharmonic parametric resonances in the new type of transition, this type of disintegration of laminar flow is usually referred to in the literature as the "subharmonic" regime.

However, in accordance with the resonance-wave concept of disintegration proposed in [1, 2] and confirmed directly in [15], parametric resonances of the subharmonic type also play the main role in the formation of the K-regime bumps. However, in this case we are dealing not with a single resonance, but with a system of resonances which intensifies deterministic initiating waves that are coherent with the main wave. In light of this, the term "subharmonic" can be used with the same (or even greater) degree of justification in regard to the K-regime of transition. Its use to denote a new regime is very unfortunate.

Novosibirsk. Translated from Zhurnal Prikladnoi Mekhaniki i Tekhnicheskoi Fiziki, No. 2, pp. 83-94, March-April, 1990. Original article submitted January 18, 1989.

0021-8944/90/3102-0239$12.50

Taking into account that the given new regime was first empirically detected in [4] and analyzed in detail in [9, 10, 13, 14] in Novosibirsk, the author of [2] proposed referring to it by the abbreviated name of the "N-regime" of disintegration. We will use this terminology below. Although it has been more than 30 yrs since the K-regime was discovered in [3], its nature (in contrast to that of the N-regime) has for the most part remained misunderstood until recently.

Experiments in [16, 17], involving detailed study of the initial stages of the K-regime (up to the formation of the characteristic bumps and their doubling and tripling), led to a reexamination of representations on certain governing disintegration mechanisms and yielded the first systematic information on the spectral (frequency and frequency-wave) structure of the perturbation field. Proceeding on the basis of an analysis of these and other results of studies, the authors of [1, 2] then proposed and indirectly substantiated the "resonance-wave concept" of the K-regime of boundary-layer disintegration. This theory explains (at least qualitatively) nearly all of the main features of the behavior of the perturbation field that are seen in experiments.

The most popular explanation for the bumps at the beginning of boundary-layer turbulence for the last 30 yrs has been local high-frequency secondary (LHS) flow instability leading to intensive reinforcement of high-frequency background disturbances due to the appearance of highly unstable, multibranched inflected velocity profiles in finite space and time regions. A large number of theoretical studies and one experimental study [18] (see [19, 20] for surveys) has been devoted to the study of the concept of LHS instability. However, the limited number of sufficiently thorough experimental studies that had been conducted made it impossible to define the role of LHS instability in the transition to turbulence. A final answer to this question was obtained in [19]. First of all, it was shown that – in contrast to the opinion most widely held – intensification of the characteristic bumps on the velocity oscillograms (which play the main role in the K-regime) does not occur under the influence of LHS instability, since none of the criteria for the realization of this type of instability are met. Secondly, intensification of considerably weaker high-frequency wave packets was seen in the flow. According to all of the criteria used, these packets corresponded to waves intensified by the mechanism of LHS instability. However, they did not have a significant effect on the breakdown of laminar flow.

The violent resonance intensification of stochastic flow oscillations seen in the N-regime of transition [9, 10] first suggested the possibility that very weak background disturbances could have a strong (resonant) effect on the transition. From the viewpoint of the resonance-wave (RW) concept of boundary-layer transition to the more complex K-regime of breakdown, first proposed in [1, 2], the main role is played by cascades (systems) of resonances which are harmonic and subharmonic (parametric) and occur between different wave trains in the frequency-wave spectrum. The existence of these systems of resonances for simple cases (two, three, and four modes) had previously been theoretically predicted in [11, 12, 21, 22] and experimentally substantiated for the case of subharmonic resonance [9, 10]. However, only in [1, 2] were these low-mode models generalized to a cascade of resonances (presumed to exist in the K-regime at the stage corresponding to the appearance of the bumps) within the framework of the RW concept and substantiated indirectly. Due to several experimental obstacles, attempts made in [16, 17] to observe this system of resonances directly were unsuccessful. Success was achieved later in additional special experiments published in [15]. It was shown that the system of harmonic and subharmonic resonance interactions postulated in [1, 2] actually exists. This result has in turn almost completely answered the question of the governing mechanisms in the initial stages of K-breakdown – to the point of the formation of the characteristic bumps on the pulsation oscillograms.

The main problems that remain in regard to understanding the K-regime of boundary-layer breakdown have to do with the subsequent (mainly after the appearance of the bumps) stages of the transition, which are characterized by the beginning of randomization of the flow. As was noted in [1, 2], due to the discovery of the deterministic nature of the bumps in [16, 17] and the still-unclear role of the mechanism of LHS instability in the intensification of random background disturbances, the question of the paths of flow randomization in the K-regime of boundary-layer transition remains unanswered.

The present study is devoted to examination of the mechanisms responsible for the appearance or intensification (from the background) of stochastic perturbations and explanation of the role of resonance interactions in the final stages of the K-regime of breakdown.

Experimental Method. Experiments were conducted in a low-turbulence subsonic wind tunnel of the T-324 type at the ITPM (Institute of Theoretical and Applied Mechanics) of the Siberian Department of the Soviet Academy of Sciences. The flow velocity in the experiment $U_\infty = 9.18$ m/sec. The conditions and methods used in the experiments (except for the method used to analyze the signals) were the same as in [10], where they were described in detail (the results reported below were obtained directly from an analysis of signals recorded on a magnetograph in 1980 and partially analyzed in [16, 17]).

Harmonic oscillations were excited in a laminar boundary layer on a flat plate by means of a vibrating ribbon located 250 mm downstream of the leading edge of the plate. A slight spatial modulation of the flow with respect to the transverse coordinate z was produced by 12.5 × 12.5 mm blocks stuck directly onto the plate under the ribbon. The spacing of the blocks $\lambda_z = 25$ mm. The initial stages of the K-regime excited by these perturbations were described in detail in [16, 17]. With the chosen amplitude and frequency ($f_1 = 96.4$ Hz) for the instability wave excited in the boundary layer, the bumps characteristic of the K-regime were formed on the pulsation oscillograms at the positions of the "peaks" along z ($\hat{z} = 2\pi z/\lambda_z = 0 \pm 2k\pi$, $k = 0, 1, 2, \ldots$), where $x \approx 440$-450 mm (x is the longitudinal coordinate reckoned from the leading edge of the plate).

The measurements were made using equipment based on a hot-wire anemometer with a linearizer [16]. The data recorded on the magnetograph was entered into the computer synchronously with the control signal recorded on the second channel of the magnetograph and corresponding to the signal fed to the vibrating ribbon — the source of the disturbances. They were analyzed on the basis of an application package which was partially described in [23]. The next section of this article describes certain stages of the analysis in greater detail.

Results of Measurements. Figure 1a shows the evolution of the oscillograms of the downstream pulsations measured at the peak of the distribution with respect to z ($\hat{z} = 0$) at a distance from the wall y = 1.0 mm. Ten synchronous realizations of pulsating flow are shown superimposed on one another for each coordinate x. The length of each realization was T for one period of the main wave. Since the disturbances are traveling waves, their phase changes (increases) with a shift downstream. This is clear from Fig. 1a. Figure 1b shows four groups of oscillograms corresponding to Fig. 1a for x = 400, 490, 510, and 550 mm but obtained after subtraction of the deterministic (periodic) component of the pulsations (which was determined by previous synchronous averaging).

The evolution of the corresponding amplitude spectra of the pulsations (width of the transmission band 4 Hz) is shown in Fig. 1c for the coordinates x = 400, 420, 450, 490, 530, and 570 mm (spectra 1-6, respectively). Each subsequent spectrum is shifted relative to the previous spectrum by +10 dB to facilitate representation of the results. Figure 1d shows curves depicting the increase in the amplitudes of the higher harmonics of the main wave $\omega_n = n\omega_1$ ($n = 1, 2, \ldots, 7$), detected in the spectra in Fig. 1c.

In the first sections (x = 400-450 mm), the oscillograms (Fig. 1a) correspond to a nearly periodic flow formed at the stage of deterministic development of space waves formed under the influence of the system of harmonic and parametric resonances described in [1, 2] from the viewpoint of the RW concept. Their spectra (Fig. 1c) consists almost exclusively of higher harmonics of the main wave; the amplitude of the pulsations of the continuous spectrum in the intervals between the harmonics is roughly two orders less than the amplitude of the deterministic components. At $x \approx 440$-450 mm, the projections characteristic of the K-regime are formed near the external boundary of the boundary layer ($y \approx 4.5$ mm). The spatial structure of the perturbations in this region was examined in detail in [16, 17, 19].

The periodic flow begins to break up farther downstream. Rapid intensification of the oscillations of the continuous spectrum are seen on the section between x = 450 and 530 mm in the pulsation spectrum (Fig. 1c). It is quite evident from the oscillograms in Fig. 1a that these oscillations have the form of the quasistochastic "wave packet" seen in the statistical sense when oscillograms are superimposed. This packet is most clearly visible for the oscillograms in Fig. 1b, where the periodic component of the process was filtered out. Although the pulsations inside the packet are unordered in character (particularly near the end of the investigated intensification region, i.e., at $x \approx 530$ mm), the packet itself has a fairly definite shape (envelope) and is located at a certain point in the period of the main wave. An increase in the x coordinate is initially accompanied by an increase in the packet's amplitude. The packet then begins to lose its distinctness and occupy an increasingly large part of the period of the main wave. Finally, at x = 550 mm, the packet nearly

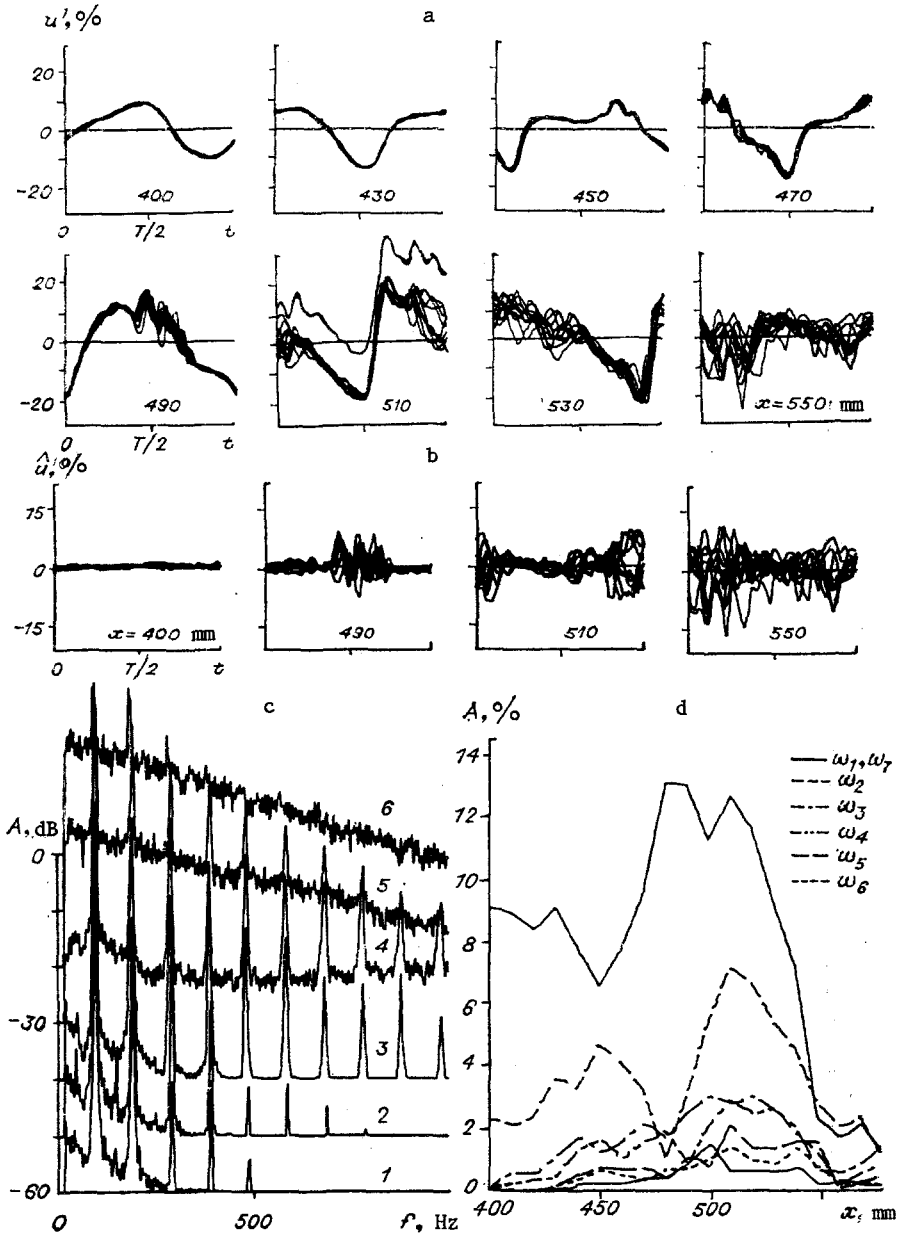

Fig. 1

ceases to exist and the oscillations lose almost all signs of periodicity. It is evident from Fig. 1d that the amplitudes of the harmonics generally increase up to x ≈ 520 mm and then begin to decrease. This decrease after attainment of a maximum is usually associated with the concluding stages of the transition to turbulence. The stage of intensification of the harmonics on the section x ≈ 470-530 mm corresponds to the formation of the semirandom wave packets, while the subsequent decay of the amplitudes corresponds to the breakup of the packets.

It should be noted that the packets are only a modulation of the intensity of the irregular pulsations undergoing reinforcement (Fig. 1b) and are not turbulence spots. One of the most obvious differences is the fact that the pulsations in the packets (in contrast to turbulence spots) do not contain high frequencies. They appear as an irregular departure of the oscillogram from its periodic trajectory on a certain section of the period of the main wave. The packet resembles a difficult section of an otherwise good road on which each driver tries to find the best path, the path on the rest of the road being well-traveled. For greater clarity, one of the series of oscillograms in Fig. 1a (at x = 510 mm) is shown separately. It is quite impossible to distinguish the packet by looking only at this oscillogram, although a turbulence spot is readily apparent on a single oscillogram.

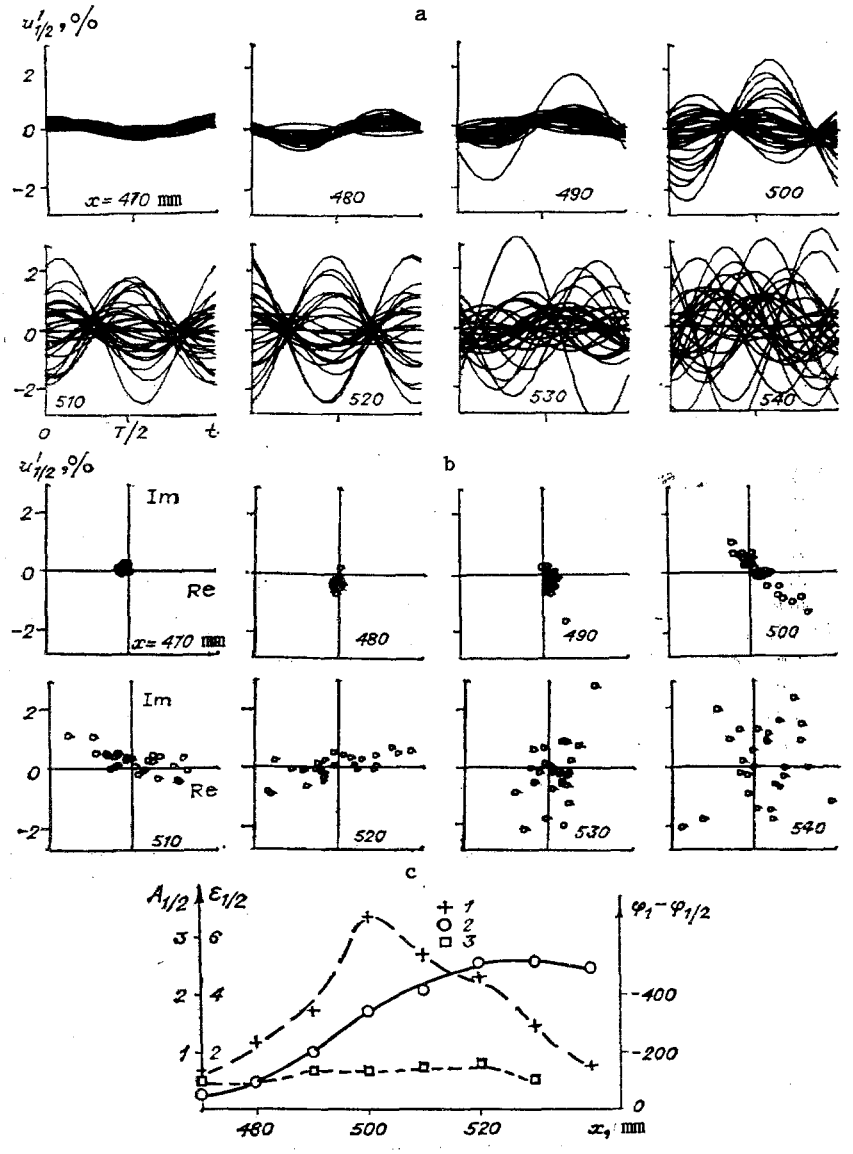

Fig. 2

Careful analysis of the oscillograms showed that none of the set of investigated points in the alternation space was observed, i.e., with regular initial conditions (with a harmonic Tollmien–Schlichting main wave causing all of the transients), as in the N-regime [3, 4, 9, 10] turbulence spots are not seen in the K-regime.

The subsequent analysis of the experimental data will be devoted to study of the mechanism responsible for the appearance of the above-noted semirandom wave packets, leading to breakdown of the periodic regime with the bumps characteristic of the K-regime boundary-layer transition.

The amplitude spectra shown in Fig. 1c do not provide any information on the phase properties of the spectral components or the evolution of the amplitudes and phases of the harmonics in a slow time scale. Such information allowed the authors of [9, 10] to elucidate the nature of N-regime of breakdown and to discover the existence of subharmonic resonances. It was predicted in [24] that, as in the N-regime, randomization of the K-regime begins with parametric resonance intensification of random background initiating perturbations. However, in the present case, this occurs not only in the region of the frequency of the subharmonic $\omega_1/2$, but also in the region of the frequencies $n\omega_1/2$ ($n = 1, 2, 3...$). The intensification takes place under the influence of a train of deterministic waves with the frequencies $n\omega_1$ formed in the K-regime at earlier stages of development [16, 17]. The qualitative scheme proposed in [2, Sec. 3.1] for the formation of quasirandom wave packets from phase-coupled wave trains also supports the proposition that the packets shown in Fig. 1, a and b,

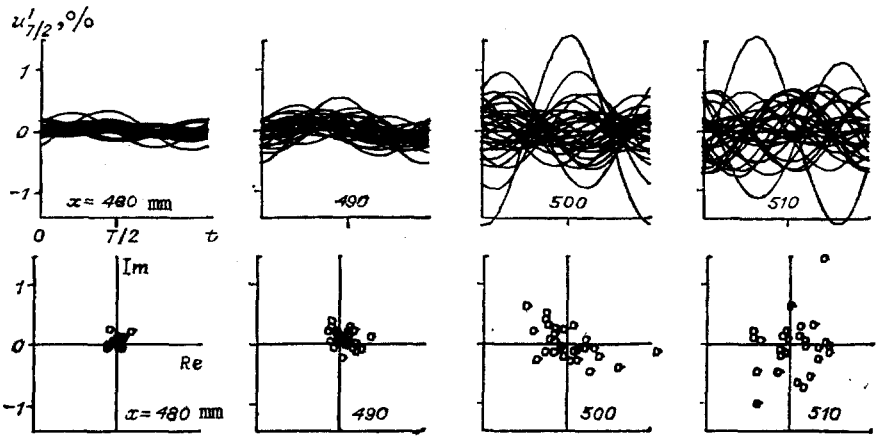

Fig. 3

are of resonant character. In other words, it is suggested that the wave packets shown in Fig. 1, a and b, are due to parametric resonance intensification of groups of semirandom subharmonic waves. The program of analysis realized below was conceived to examine the validity of this proposition.

Figure 2a shows families of pulsation oscillograms in the region of the subharmonic frequency. The oscillograms were isolated for 28 successive moments of slow time from a long realization (lasting about 10 sec). The oscillograms were obtained using a program for complex Fourier analysis in two time scales (which gives the evolution of the amplitudes and phases of the harmonics and subharmonics over slow time), with subsequent inverse Fourier transformation for a unique chosen harmonic in the spectrum (in the given case, for the subharmonic). The procedures followed for the two-scale Fourier analysis were: 1) subdivision of a long oscillogram into segments, with the beginning of the segments being time-shifted by intervals which were multiples of the period of the subharmonic and the segments having lengths which were two periods of the subharmonic; 2) weighting of each segment with a Kaiser–Bessel window; 3) fast Fourier transformation of each weighted segment with the discard of "superfluous" spectral harmonics differing from $n\omega_1/2$ and not bearing phase information; 4) normalization of the resulting amplitudes to allow for coherent intensification of the window and correction of the phases of the harmonics for the cases when the quantization time is not a multiple of the slow time step. The characteristics of Kaiser–Bessel windows were discussed in [25]. In the present case, we used the window parameter $\alpha_{qu} = 2.0$. Its equivalent-noise bandwidth was 1.5 bits. Under the conditions of the experiment conducted here, 1 bit corresponded to about 24.1 Hz. The effective passband in the Fourier analysis was thus about 36 Hz.

The graphs in Fig. 2a show that subharmonic pulsations are intensively reinforced in the region where the quasirandom wave packet appears ($x \approx 470$-520 mm) (also see Fig. 2c) and take on the characteristic form, with nodes and antinodes. This form of oscillogram corresponds to subharmonic disturbances with an amplitude which fluctuates according to a random law. The phase is nearly constant, although it changes suddenly by π at random moments of time when the amplitudes pass through zero. The points of the phase trajectory of the subharmonic pulsations corresponding to these oscillograms in the complex plane are shown in Fig. 2b. It is evident that the cloud comprised of these points – which initially corresponded to random oscillations – is stretched out into an ellipse with a semiaxis ratio which increases in value. The ellipse ultimately becomes almost a straight line whose slope gives the fixed value of the phase.

Such behavior by the subharmonic pulsations was observed earlier in [9, 10] (compare Fig. 2a and b in the present study with Fig. 5, 15-17 in [10]). However, as was shown in [9, 10], this behavior corresponds to intensification of random subharmonic background disturbances under the influence of parametric resonance with a main wave of the frequency ω_1.

Although some ordering of the pulsations occurs during the resonance intensification, they retain features of randomness. On the one hand, their "instantaneous" frequency is fixed and is equal to the frequency of the subharmonic $\omega_{1/2} = \omega_1/2$, while their phase takes only two values: φ_r and $\varphi_r + \pi$, where φ_r is the resonance value of the phase determined by the difference between the phases of the subharmonic and the main wave in accordance with

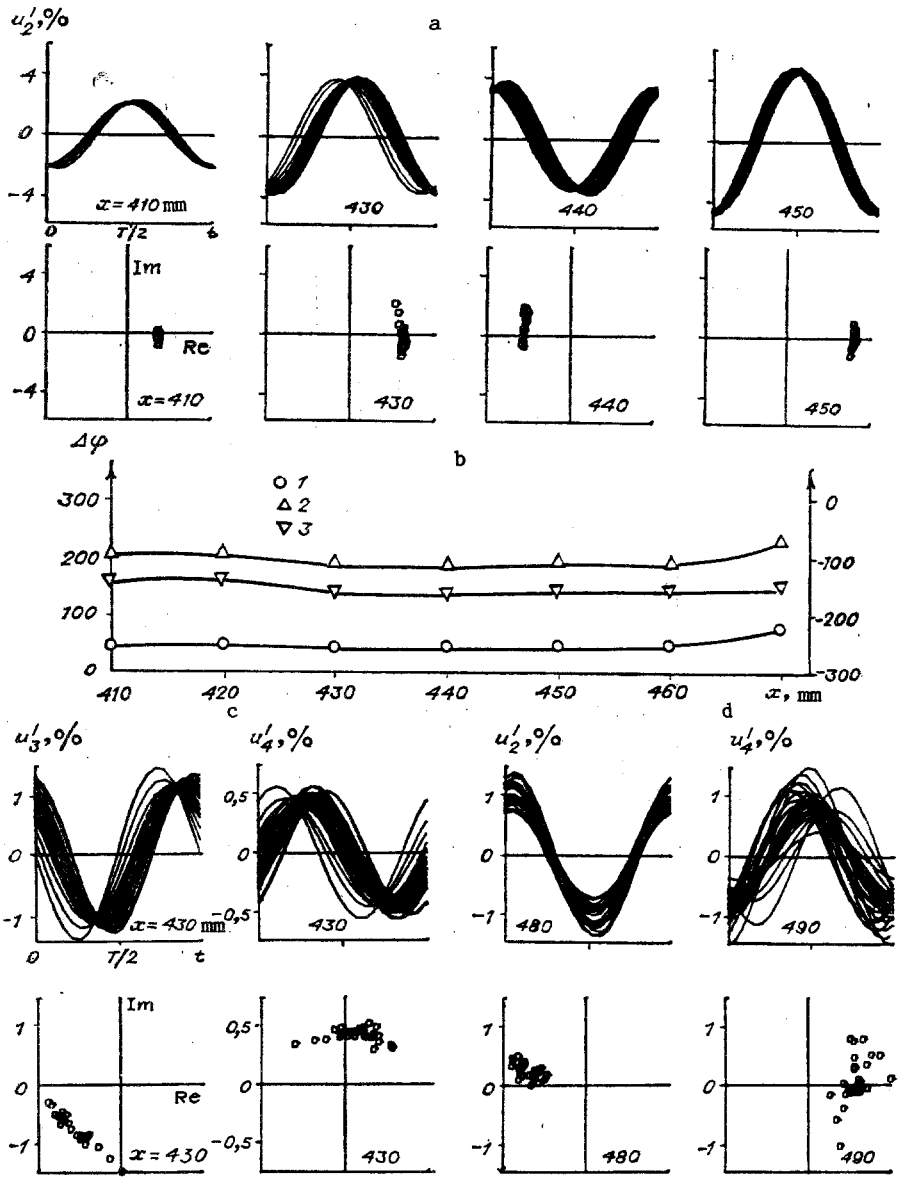

Fig. 4

the condition of resonance phase synchronism (see [9, 10]). On the other hand, the random behavior of the amplitude and the random moments of time at which the phase jumps take place have a stochastic element which is "inherited" from the initial background disturbances. As a result, when the Fourier analysis is performed for long periods of time, these oscillations correspond to a broad section of the continuous spectrum in the region of the subharmonic frequency. The ability of subharmonic resonance to amplify disturbances within a broad range of the continuous spectrum was described, studied, and explained on the basis of quasi-steady principles in [9, 10] and is consistent with the extremely large spectral width of the resonance.

Figure 2c demonstrates the connection between the amplitude $A_{1/2}$ of the semirandom subharmonic undergoing amplification and the degree of elongation of the cloud of points of its phase trajectory $\varepsilon_{1/2} = a/b$ (a and b are the dimensions of the cloud along its principal axes). Also shown is the connection between the amplitude of the subharmonic and the difference between its phase and the phase of the main wave ($\varepsilon_{1/2}$, $A_{1/2}$, $\varphi_1 - \varphi_{1/2}$ correspond to graphs 1-3). It is apparent that the highest amplification rates correspond to the largest cloud elongations due to resonance. Phase synchronism of the subharmonic and the main wave is also seen in the resonance region. It should be noted that signs of resonance disappear in the region x ≈ 520-530 mm, and there is a simultaneous stop to further increases in the amplitude of the subharmonic (the same is true of the packet integrated over the spectrum).

Thus, it has been found that flow randomization in the K-regime begins (analogously to the N-regime) with the parametric resonance intensification of a broad continuous spectrum of subharmonic pulsations in the region of the frequency $\omega_{1/2}$. However, as noted above, since the spectrum contains a broad series of high-amplitude higher harmonics of the main wave, all of the necessary conditions are created in the K-regime for the appearance of not one but a whole system of parametric resonances. An analysis shows that such a system actually exists.

Figure 3 shows oscillograms and points of phase trajectories of pulsations in the frequency region $\omega_{7/2} = 7\omega_{1/2}$. These oscillograms are analogous to those shown in Fig. 2. It is apparent that, as in the case of the subharmonics, resonance intensification of semirandom perturbations again takes place. This is manifest in a characteristic extension of the phase trajectories into an ellipse and the formation of the corresponding nodes and antinodes on the oscillograms at the moments of rapid increase in the amplitudes of the perturbations and the appearance of quasirandom "wave packets" on the integral oscillograms of the pulsations. Similar resonance phenomena were recorded in the region of other subharmonics with frequencies around $(2k + 1)\omega_1/2$ ($k = 0, 1, 2, \ldots, 6$). However, it is evident that the oscillations which force the waves at the frequencies $n\omega_1$ should have odd numbers $n = 2k + 1$. Even harmonics with the frequencies $2m\omega_1$ ($m = 1, 2, 3\ldots$) may also cause resonance intensification of stochastic pulsations on sections of the continuous spectrum around the frequencies $2m\omega_1/2 = m\omega_1$ ($m = 1, 2, 3\ldots$), as was seen here.

Figure 4a shows oscillograms and points of phase trajectories for the early stages of development of the perturbations in the region of the frequency $\omega_2 = 2\omega_1$. The main difference between these disturbances and those shown in Figs. 2 and 3 is that the characteristic nonperiodic background disturbances that are intensified by parametric resonance and lead to the characteristic nodes and antinodes on the oscillograms are superimposed on a periodic deterministic wave of the frequency ω_2. The cloud of points of the phase trajectory is again extended almost into straight lines. In the given case, these lines are shifted far from the origin and are "seated" on the end of the vector corresponding to the deterministic wave of frequency ω_2, the amplitude and phase of this wave being nearly constant over time. Disturbances having similar properties are seen in the region of other frequencies of the type $m\omega_1$; examples for ω_3 and ω_4 are shown in Fig. 4c and d.

To eliminate the "shielding" effect of high-amplitude periodic components of the pulsations when studying irregular oscillations in the region of the frequencies $m\omega_1$ ($m = 1, 2, 3\ldots$), we separated the noncoherent part of the perturbations from the coherent part with the main wave by synchronous subtraction of the periodic component (obtained by summing a large number of realizations) from the integral signal. Figure 1b gives examples of oscillograms of such irregular components, while Fig. 5 shows typical narrow-band oscillograms and the corresponding phase-trajectory points for oscillations in the region of the frequencies ω_1, ω_2, ω_3, ω_4, ω_5, and ω_7 at $x = 450$ (*a*) and 470-480 mm (b).

Comparison of the graphs for ω_2 at $x = 450$ and 480 mm in Fig. 5 and Fig. 4a and d, clearly demonstrates the effect of eliminating the periodic component. The narrow-band oscillograms lose their sinusoidal component and become similar to those seen for oscillations in the region of the frequencies $(2k + 1)\omega_1/2$ (see Figs. 2 and 3). The cloud of phase-trajectory points is shifted in this case, with its center lying at the origin.

It should be noted that, in principle, the observed intensification of the stochastic addition to deterministic perturbations for the special case of perturbations around the frequency ω_1 (Fig. 5a) corresponds to the phenomenon of modulation instability familiar from the theory of vibration [26], i.e., it corresponds to parametric resonance between the harmonic $2\omega_1$ and weak disturbances around the frequency ω_1, leading to slow modulation of its amplitude and phase. However, the number of waves that actually participates in the interaction in the K-regime is of course considerably greater.

The phase-trajectory points in Fig. 4a demonstrate the constancy of the phase shift between the deterministic periodic oscillations at the frequency $2\omega_1$ and the semirandom nonperiodic oscillations in the region of this frequency (if the phase jumps of the latter by π are not taken into account). The phase of the first oscillations corresponds to the angle of rotation of the vector connecting the coordinate origin and the center of the cloud of phase-trajectory points. The phase of the second oscillations is determined by the direction along which the cloud is extended. This property is manifest in Fig. 4a through synchronous rotation of the first and second phases as downstream shifts occur, which is a situation re-

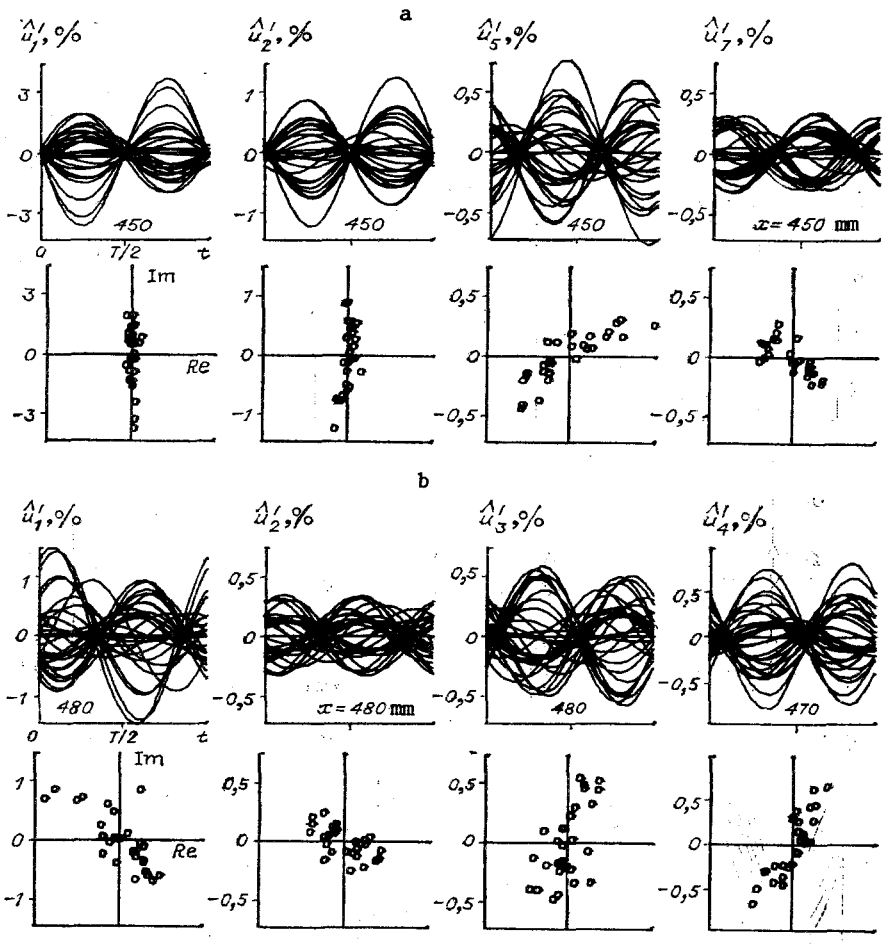

Fig. 5

sembling the rotation of the moon about the earth (with the same side always facing the earth). Figure 4b (curve 1) shows the dependence of the corresponding phase difference between the deterministic and stochastic perturbations $\varphi_{2d} - \varphi_{2s}$. The same property is manifest for oscillations occurring in the region of higher-frequency harmonics, particularly for ω_3, ω_4, ω_5, ω_6.

Such phase synchronization is an expected consequence of the fact that deterministic (coherent with the main wave) and stochastic (noncoherent with ω_1) initiating oscillations are intensified simultaneously and probably independently by the same mechanism of parametric resonance under the influence of the same forcing waves (this is the wave ω_4 for Fig. 4a and b). The linearity of the parametric resonances – in the sense of satisfaction of the principle of superposition for the intensified subharmonic perturbations and the absence of their inverse effect on the forcing wave – was demonstrated in [9, 10] and observed up to very large subharmonic amplitudes, i.e., up to amplitudes 2.4 times greater than the amplitudes of the forcing wave! The graphs in Fig. 4b actually show the satisfaction of synchronism conditions for both types of pulsations reinforced in the region of the frequency $2\omega_1$ with oscillations at the frequency of the forcing wave $4\omega_1$. The phase differences $\varphi_{4d} - \varphi_{2d}$ (curve 2) and $\varphi_{4d} - \varphi_{2s}$ (curve 3) in this region remain nearly constant (d and s in the subscripts denote the deterministic and stochastic components of the oscillations, while the figures denote the corresponding numbers of the harmonics).

It should be noted that the intensification of noncoherent (with the main wave) pulsations in the region of the frequency ω_2, shown in Fig. 4a, occurs at earlier stages of development than for stochastic perturbations in the frequency region $\omega_{1/2}$, $\omega_{7/2}$, shown in Figs. 2 and 3. The same occurs for the noncoherent pulsations around the frequencies ω_3, ω_4 (Fig. 4c) and ω_1, ω_5, ω_7 (Fig. 5a). However, a new type of intensification of these oscillations is seen downstream, the peak here – as for all the other cases – being seen in the region x ≈ 470-520 mm. Figure 4d shows the moments of intensification, with manifestation of the characteristic signs of parametric resonance, for disturbances near the harmonics ω_2 and ω_4. The same is shown in Fig. 5b for ω_1, ω_3, ω_4.

We examined the reasons for the earlier manifestation of the resonance amplification of certain noncoherent perturbations in the region of the frequencies ω_1, ω_2, ω_3, ω_4, etc. It turned out that the perturbations amplified in the region x = 400-450 mm, although noncoherent with ω_1, are fairly regular in character and are connected with the slight deviation of the output signal of the generator (fed to the vibrating ribbon) from strict sinusoidal shape. The signal contains distortions caused by network induction and manifest in slight modulation of its amplitude over time with the frequency $\Delta f = 2f_i - f_1$ ($f_i \approx 50$ Hz is the frequency of the network induction). Such modulation corresponds to the presence of very small oscillations at the frequencies $f_1 \pm \Delta f$ in the spectrum. However, these oscillations were greater in amplitude than the background perturbations, which were different in nature. Thus, it is these oscillations that act as initiating oscillations in the frequency region $n\omega_1$ (n = 1, 2, 3...) at the first stage of resonance intensification of noncoherent perturbations. The weaker stochastic background perturbations have to move to a greater distance downstream in order for the resonances to strengthen them to detectable amplitudes and make them distinguishable from the background of perturbations of another type. This second stage of amplification took place for all of the investigated subharmonic (in the broad sense) disturbances at approximately x = 470-520 mm. Here, the property of linearity of the parametric resonances was manifest to a greater extent than in the case of the amplified disturbances discussed above and observed in [9, 10].

It should be noted that the process of the resonance intensification of disturbances in the flow cannot of course continue indefinitely. It is quite evident from Figs. 2, 3a, and 4a that the stage of intensive amplification is replaced by a slow stage and cessation of amplitude growth, with simultaneous loss of phase synchronism and gradual disappearance of the extension of the cloud of phase-trajectory points along the direction of the resonance phase. In the same way, the resonances complete most of their work on the deterministic initiating oscillations coherent with the main wave, in accordance with the formation of the bumps on the oscillograms, by the point x ≈ 460 mm (see [1, 2, 15-17, 19]).

Thus, an analysis of the intensification of perturbations of the continuous spectrum that are noncoherent with the main wave has shown that, as in the N-regime, the main reason for the beginning of randomization of flow in the K-regime of boundary-layer transition is the parametric resonance amplification of random background initiating perturbations of the boundary layer near the frequencies of the subharmonics of the corresponding deterministic forcing waves. In contrast to the N-regime, in the K-regime there is the simultaneous realization of a whole system of parametric subharmonic resonances based on different deterministic forcing waves with the frequencies $n\omega_1$ intensified at earlier (in the case of the K-regime) stages of the transition – at the stage of formation of the periodic bumps on the oscillogram. Since subharmonic resonances which are of the same type but which intensify deterministic initiating oscillations play the main role in the generation of periodic secondary flows with bumps [1, 2, 15-17], it can be concluded that the same event that engenders this flow is also the cause of its breakdown. The competition between resonance breakdown of the flow (with the intensification of stochastic initiating background oscillations) and the resonance generation of the bumps (during the intensification of initiating oscillations that are coherent with the main wave) also determines whether the K-regime or the N-regime will prevail, as well as all possible intermediate types of breakdown of a laminar boundary layer. Although the mechanism of flow randomization in the K-regime requires more detailed study, at the current stage of investigation it can be definitively concluded that the hypothesis advanced in [24] regarding the main causes of randomization in the K-regime of boundary-layer transition has been substantiated.

LITERATURE CITED

1. Yu. S. Kachanov, "Resonance-wave nature of the transition to a turbulent boundary layer," in: Modeling in Mechanics [in Russian], Vol. 1 (18), No. 2, ITPM, Sib. Otd., Akad. Nauk SSSR (1987).
2. Yu. S. Kachanov, "On the resonant nature of the breakdown of a laminar boundary layer," J. Fluid Mech., 184, 43 (1987).
3. P. S. Klebanoff, K. D. Tidstrom, and L. M. Sargent, "The three-dimensional nature of boundary-layer instability," J. Fluid Mech., 12, Pt. 1 (1962).
4. Yu. S. Kachanov, V. V. Kozlov, and V. Ya. Levchenko, "Nonlinear development of a wave in a boundary layer," Izv. Akad. Nauk SSSR Mekh. Zhidk. Gaza, No. 3 (1977).
5. Yu. S. Kachanov, V. V. Kozlov, and V. Ya. Levchenko, Generation of Turbulence in a Boundary Layer [in Russian], Nauka, Novosibirsk (1982).

6. W. S. Sarle, J. D. Carter, and G. A. Reynolds, "Computation and visualization of unstable-wave streamlines in a boundary layer," Bull. Am. Phys. Soc., 26, 1252 (1981).
7. A. S. W. Thomas and W. S. Sarle, "Harmonic and subharmonic waves during boundary-layer transition," Bull. Am. Phys. Soc., 26, 1252 (1981).
8. W. S. Sarle, V. V. Kozlov, and V. Ya. Levchenko, "Forced and unforced subharmonic resonance in boundary-layer transition," AIAA Pap., No. 84-0007 (1984).
9. Yu. S. Kachanov and V. Ya. Levchenko, "Resonance interaction of perturbations with the transition to turbulence in a boundary layer," Preprint ITPM Sib. Otd. Akad. Nauk SSSR, No. 10-82, Novosibirsk (1982).
10. Yu. S. Kachanov and V. Ya. Levchenko, "The resonant interaction of disturbances at laminar-turbulent transition in a boundary layer," J. Fluid Mech., 138, 209 (1984).
11. G. S. Raetz, "A new theory of the case of transition to turbulent flows," Norair Rep.; NOR - 59-383, Hawthorne, CA (1959).
12. A. D. D. Craik, "Nonlinear resonant instability in boundary layers," J. Fluid Mech., 50, Pt. 2 (1971).
13. A. G. Volodin and M. B. Zel'man, "Three-wave resonance interaction of disturbances in a boundary layer," Izv. Akad. Nauk SSSR Mekh. Zhidk. Gaza, No. 5 (1978).
14. M. B. Zel'man and I. I. Maslennikova, "Resonance interaction of three-dimensional disturbances in a boundary layer," in: Instability of Sub- and Supersonic Flows [in Russian], ITPM Sib. Otd. Akad. Nauk SSSR, Novosibirsk (1982).
15. V. I. Borodulin and Yu. S. Kachanov, "Cascade of harmonic and parametric resonances in the K-regime of boundary-layer transition," Model. Mekh., ITPM Sib. Otd. Akad. Nauk SSSR, 3(20), No. 2 (1989).
16. Yu. S. Kachanov, V. V. Kozlov, V. Ya. Levchenko, and M. P. Ramazanov, "Experimental study of the K-regime of boundary-layer transition," Preprint ITPM Sib. Otd. Akad. Nauk SSSR; No. 9-84, Novosibirsk (1984); Yu. S. Kachanov, V. V. Kozlov, V. Ya. Levchenko, and M. P. Ramazanov, "Nature of the K-breakdown of a laminar boundary layer," Izv. Akad. Nauk SSSR, Ser. Tekh. Nauk, 2, No. 7 (1989).
17. Yu. S. Kachanov, V. V. Kozlov, V. Ya. Levchenko, and M. P. Ramazanov, "On nature of K-breakdown of a laminar boundary layer. New experimental data," in: Laminar-Turbulent Transition: Symp. Novosibirsk, USSR (1984), Springer, Berlin et al. (1985).
18. M. Nishioka, M. Asai, and S. Iida, "An experimental investigation of the secondary instability," in: Laminar-Turbulent Transition: Symp., Stuttgart, FRG (1979), Berlin et al., Springer (1980).
19. V. I. Borodulin and Yu. S. Kachanov, "Role of the mechanism of local secondary instability in relation to the K-breakdown of a boundary layer," Izv. Sib. Otd. Akad. Nauk SSSR Ser. Tekh. Nauk, 5, No. 18 (1988).
20. A. H. Nayfeh, "Nonlinear stability of boundary layers," AIAA Pap., No. 87-0044 (1987).
21. A. H. Nayfeh and A. N. Bozatli, "Nonlinear wave interactions in boundary layers," AIAA Pap., No. 79-1493 (1979).
22. A. H. Nayfeh and A. N. Bozatli, "Nonlinear interaction of waves in boundary-layer flows," VPI and SU Rep. NVPI - E - 79.6 (1979).
23. Yu. S. Kachanov, "Complex of programs for two-dimensional and two-scale Fourier analysis of data and its use in the study of problems of turbulence generation," in: Promising Methods of Planning and Analyzing Experiments in the Study of Random Fields and Processes [in Russian], Vol. 2, MEI, Moscow (1985).
24. Yu. S. Kachanov, "Resonance breakdown of a laminar boundary layer," in: Current Problems of Ship Hydrodynamics and Aerodynamics [Russian translation], Bolgar. Inst. Gidrodinamiki Sudna, Varna, Vol. 3 (1985).
25. F. J. Harris, "Use of windows in harmonic analysis by the method of discrete Fourier transform," TIIER, 66, No. 1 (1978).
26. G. B. Whitham, Linear and Nonlinear Waves, Wiley, New York (1974).